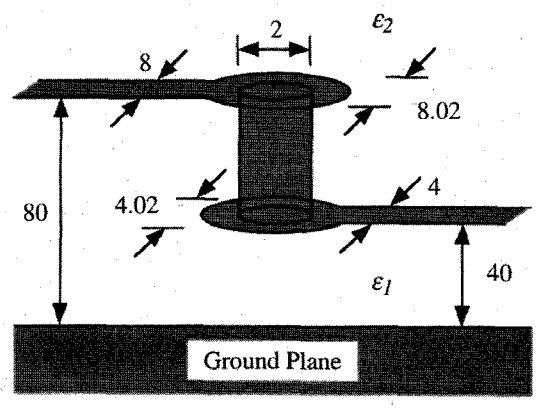

(a)

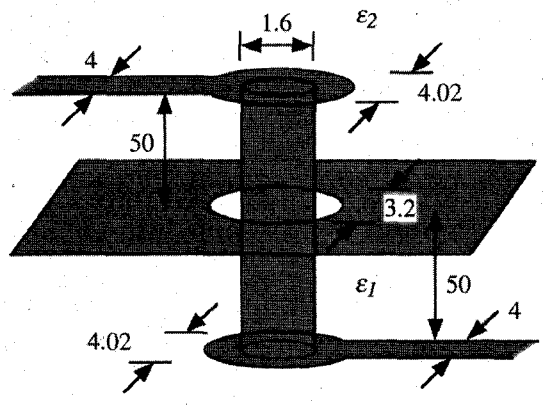

(b)

Fig. 3. (a) A two-trace via with a reference plane and (b) a two-trace via with a reference conductor. All dimensions are in mm.

excess capacitances for Fig. 3(a) with 1) $\varepsilon_1 = \varepsilon_2 = \varepsilon_0$ and 2) $\varepsilon_1 = 4\varepsilon_0$ and $\varepsilon_2 = \varepsilon_0$; for Fig. 3(b) with 3) $\varepsilon_1 = \varepsilon_2 = 4\varepsilon_0$ and 4) $\varepsilon_1 = 4.5\varepsilon_0$ and $\varepsilon_2 = 5.4\varepsilon_0$ are listed in Table I along with data obtained from [1] and [3]. In [1] and [3], the strips were replaced by the equivalent wires of radii which are one-fourth of the widths of the strips. In our computation, the lengths of all traces have been truncated to $2.5h$, whereas the width of the reference conductor has been truncated to $1.5l$, with h and l being the height of a via hole and the length of the traces. The truncation of traces and reference conductors is valid since the excess charge distribution decays rapidly as we move away from the center of a via. A total of 263 and 687 unknowns were used for the vias shown in Figs. 3(a) and (b), respectively. As shown in Table I, the data for the via shown in Fig. 3(a) agree well with the published results. However, the data for the via shown in Fig. 3(b) are considerably different from the results reported elsewhere. Unfortunately, no experimental result for this structure is available to establish the relative accuracy of these results associated with Fig. 3(b).

V. Conclusion

A method to compute the equivalent capacitance of a via, which is based on an integral equation formulated in terms of the excess charge formulation, has been presented in this paper. The method is applicable to via geometries with or without through-hole reference conductors. The recently developed closed-form Green's function was employed to circumvent the time-consuming evaluation of a nested infinite series, required in the evaluation [3].

References

[1] T. Wang, R. F. Harrington, and J. R. Mautz, "Quasi-static analysis of a microstrip via through a hole in a ground plane," *IEEE Trans. Microwave Theory Tech.*, vol. 36, pp. 1008–1013, June 1988.

[2] P. Kok and D. De Zutter, "Capacitance of a circular symmetric model of a via hole including finite ground plane thickness," *IEEE Trans. Microwave Theory Tech.*, vol. 39, pp. 1229–1234, July 1991.

[3] T. Wang, J. R. Mautz, and R. F. Harrington, "The excess capacitance of a microstrip via in a dielectric substrate," *IEEE Trans. Computed-Aided Design*, vol. 9, pp. 48–56, Jan. 1990.

[4] Q. Gu, Y. E. Yang, and M. A. Tassoudji, "Modeling and analysis of vias in multilayered integrated circuits," *IEEE Trans. Microwave Theory Tech.*, vol. 41, pp. 206–214, Feb. 1993.

[5] Q. Gu, M. A. Tassoudji, S. Y. Poh, R. T. Shin, and J. A. Kong, "Coupled noise analysis for adjacent vias in multilayered digital circuits," *IEEE Trans. Circuit Syst.*, vol. 41, pp. 796–804, Dec. 1994.

[6] Y. L. Chow, J. J. Yang, and G. E. Howard, "Complex images for electrostatic field computation in multilayered media," *IEEE Trans. Microwave Theory Tech.*, vol. 40, pp. 1120–1125, July 1991.

[7] K. S. Oh, D. Kuznetsov, and J. E. Schutt-Aine, "Capacitance computations in a multilayered dielectric medium using closed-form spatial Green's functions," *IEEE Trans. Microwave Theory Tech.*, vol. 42, pp. 1443–1453, Aug. 1994.

[8] K. S. Oh, "Efficient modeling of interconnections and capacitive discontinuities in high-speed digital circuits," Ph.D. dissertation, Univ. of IL at Urbana-Champaign, 1995.

[9] A. R. Djordjevic and T. K. Sarkar, "Computation of inductance of simple vias between two striplines above a ground plane," *IEEE Trans. Microwave Theory Tech.*, vol. 33, pp. 265–269, Mar. 1985.

Analysis of Edge Coupled Strip Inset Dielectric Guide

Z. Fan and Y. M. M. Antar

***Abstract*—The edge coupled strip inset dielectric guide is analyzed using the extended spectral domain approach. This structure, as compared to microstrip line, has several interesting features and can be very useful for microwave and millimeter wave applications. Validity of the approach is established by comparing numerical results with measured data. As many structural and material parameters can be chosen, a wide fundamental mode bandwidth and a broad range of characteristic impedances can be achieved, leading to great flexibility. The dispersion in fundamental mode propagation constants and impedances is found to be very low. With suitable choice of different permittivities for two dielectric layers, the same propagation constants for two fundamental modes can be obtained. This property is desirable for directional coupler applications.**

I. Introduction

Microstrip line has been the most popular transmission medium used for constructing microwave and millimeter wave circuits [1]. It is well known that one of the problems with open microstrip circuits is the excitation of surface waves from discontinuities in the circuits

Manuscript received July 26, 1995; revised November 12, 1995.

The authors are with the Department of Electrical and Computer Engineering, Royal Military College of Canada, Kingston, ON K7K 5L0, Canada.

Publisher Item Identifier S 0018-9480(96)01462-7.

[2]. Surface waves cause stray coupling between components and may degrade circuit performance. However, the propagation of the surface waves can be prevented if the microstrip circuit is housed within an inset dielectric guide (IDG) [3]. Furthermore, the electrical characteristics can be controlled by the dimensions of the IDG and the location of the circuit. This has resulted in the recent developments of several novel waveguide structures [4]–[7]. They include microstrip loaded IDG, embedded strip IDG, and broadside coupled strip IDG. In this paper, a new IDG structure, edge coupled strip IDG, is proposed for the application to components such as directional couplers, and analyzed by the extended spectral domain approach. As shown in Fig. 1, this structure consists of two parallel conducting strips which are placed between two dielectric layers inside the IDG groove. In comparison with open edge coupled microstrip line, this IDG structure offers several advantages: good confinement of the fields in the groove, suppression of propagation of surface modes, reduction of electromagnetic interference by side walls of the groove, lower radiation loss at discontinuities, and additional degrees of freedom to obtain characteristic parameters.

II. Analysis

The spectral domain approach has been extended to analyze a broadside coupled strip IDG, and its good efficiency and accuracy have been demonstrated [7]. This extended approach is applied here to treat the edge coupled strip IDG and to obtain propagation constants and characteristic impedances. First, discrete and continuous Fourier transforms are used to represent the fields in groove and air regions, respectively. Then, by enforcing the conditions that the tangential magnetic field components at $y = 0$ are continuous for $|x| < \frac{a}{2}$ and that the tangential electric field components at $y = -h_1$ vanish for $\frac{s_2}{2} < |x| < \frac{s_2}{2} + w_2$, we obtain four integral equations for the tangential electric field components $\left(E_x^u,\ \frac{\partial E_z^u}{\partial x}\right)$ at $y = 0$ and the current components $\left(\frac{\partial J_x^l}{\partial x},\ J_z^l\right)$ at $y = -h_1$. Next, expanding E_x^u, $\frac{\partial E_z^u}{\partial x}$, $\frac{\partial J_x^l}{\partial x}$, and J_z^l in terms of known basis functions and taking the inner product of the integral equations with basis functions leads to a homogeneous matrix equation for the unknown expansion coefficients. Setting the determinant of the coefficient matrix to be zero results in the determinantal equation for the propagation constants. To obtain fast convergence of the solutions, the edge conditions satisfied by E_x^u, $\frac{\partial E_z^u}{\partial x}$, $\frac{\partial J_x^l}{\partial x}$, and J_z^l should be incorporated into a complete set of orthogonal basis functions. Since the metallic corners of the groove and the edges of the conducting strips introduce singularity of type $r^{-\frac{1}{3}}$ in E_x^u, $\frac{\partial E_z^u}{\partial x}$ and type $r^{-\frac{1}{2}}$ in $\frac{\partial J_x^l}{\partial x}$ and J_z^l, respectively, the following basis functions are chosen

$$E_{xm}^u(x) = \frac{\partial E_{zm}^u(x)}{\partial x} = \frac{1}{N_n^C}\left[1 - \left(\frac{2x}{a}\right)^2\right]^{-\frac{1}{3}} \times C_n^{\frac{1}{6}}\left(\frac{2x}{a}\right) \quad \text{for } |x| < \frac{a}{2} \tag{1}$$

where $C_n^{\frac{1}{6}}$ are Gegenbauer polynomials, and N_n^C are normalization factors. $n = 2m$ and $n = 2m + 1$ are chosen for the E_z odd and even modes, respectively. Note that $m = 0, 1, 2 \cdots$ except that $m = 1, 2, \cdots$ for $\frac{\partial E_{zm}^u}{\partial x}$ for the E_z odd mode since the zeroth term of $E_z^u(x)$ for the E_z odd mode is not zero at the metallic corners as the boundary condition for $E_z^u(x)$ requires

$$\frac{\partial J_{xm}^l(x)}{\partial x} = J_{zm}^l(x) = \frac{1}{N_n^T}(1 - x'^2)^{-\frac{1}{2}} \times \begin{cases} T_m(x') & \text{for } \frac{s_2}{2} < x < \frac{s_2}{2} + w_2 \\ \pm T_m(x') & \text{for } -\frac{s_2}{2} - w_2 < x < -\frac{s_2}{2} \end{cases} \tag{2}$$

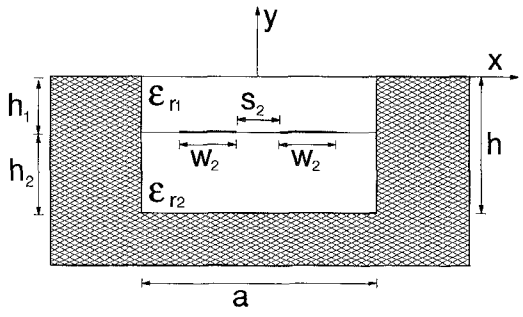

Fig. 1. Cross section of an edge coupled strip inset dielectric guide.

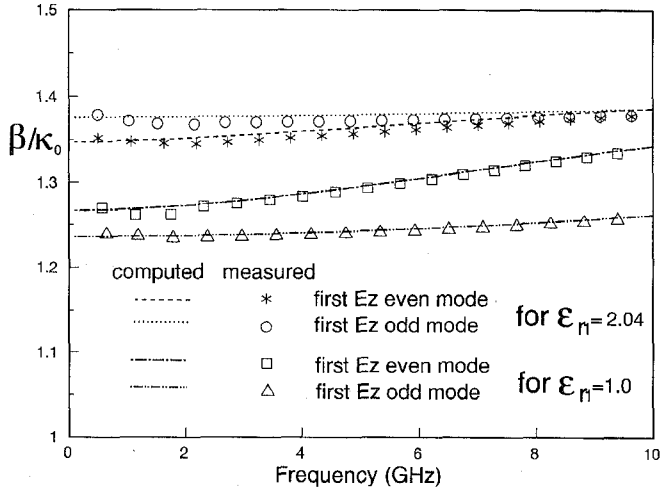

Fig. 2. Computed and measured propagation constants of the first E_z even and odd modes ($\varepsilon_{r2} = 2.04$, $a = 22.86$ mm, $h_1 = 2.16$ mm, $h_2 = 8$ mm, $w_2 = 5$ mm, $s_2 = 3$ mm).

where T_n are Chebyshev polynomials, N_n^T are normalization factors, and $x' = 2(|x| - x_0)/w_2$, $x_0 = (s_2 + w_2)/2$. The plus and minus signs $\pm$ in (2) are chosen for the E_z even and odd modes, respectively. m is chosen to start at zero for $J_{zm}^l(x)$, but at one for $\frac{\partial J_{xm}^l(x)}{\partial x}$. This is because the $m = 0$ term is not zero at the edges of conducting strips as the boundary condition for $J_x^l(x)$ requires. Finally, based on the total transported power and the longitudinal strip currents, characteristic impedances of two fundamental modes are calculated.

III. Results and Discussions

To verify the accuracy of the analysis presented in the previous section, measurements were performed for comparison with computed results. The resonant section method was used to measure propagation constants. Fig. 2 shows the comparison of the computed and measured propagation constants of the first E_z even and odd modes. Clearly, the agreement between computed and measured data is good.

Fig. 3 shows the propagation constants of the first and second E_z even and odd modes as a function of frequency up to 40 GHz. It is clear that the two fundamental modes with no cutoff frequency are the first E_z even and odd modes. In this case, the first higher-order mode is the second E_z odd mode, whose finite cutoff frequency determines the fundamental mode bandwidth where only two fundamental modes can propagate. It should be noted that the first higher-order mode can be either second odd or even mode depending on the IDG dimensions. The cutoff frequency of the first higher-order mode can be controlled by changing the dimensions of the IDG. The propagation constants

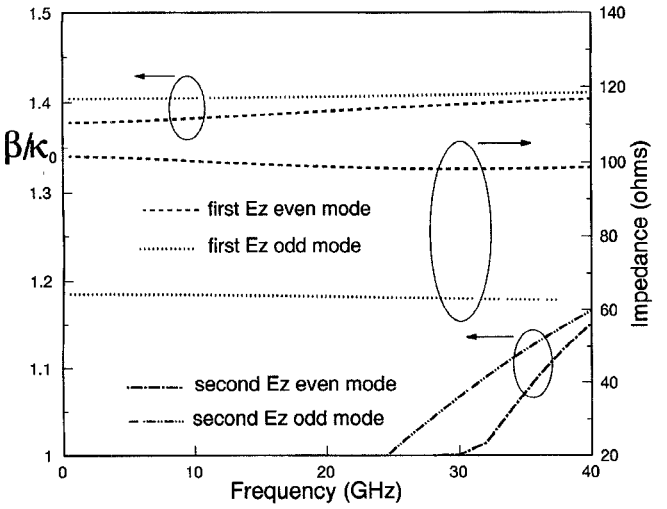

Fig. 3. Propagation constants of the first and second E_z even and odd modes, and characteristic impedances of first E_z even and odd modes as a function of frequency ($\varepsilon_{r1} = \varepsilon_{r2} = 2.04$, $a = 6$ mm, $h_1 = 1$ mm, $h_2 = 2$ mm, $w_2 = 1.5$ mm, $s_2 = 1$ mm).

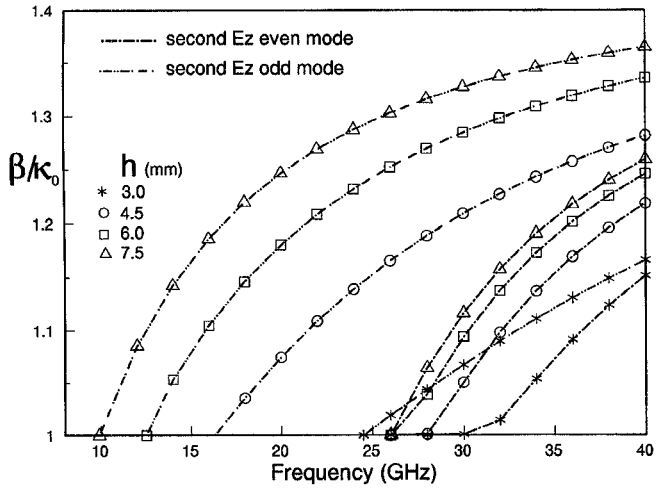

Fig. 4. Propagation constants of the second E_z even and odd modes as a function of frequency for different values of h ($\varepsilon_{r1} = \varepsilon_{r2} = 2.04$, $a = 6$ mm, $h_1 = 1$ mm, $w_2 = 1.5$ mm, $s_2 = 1$ mm).

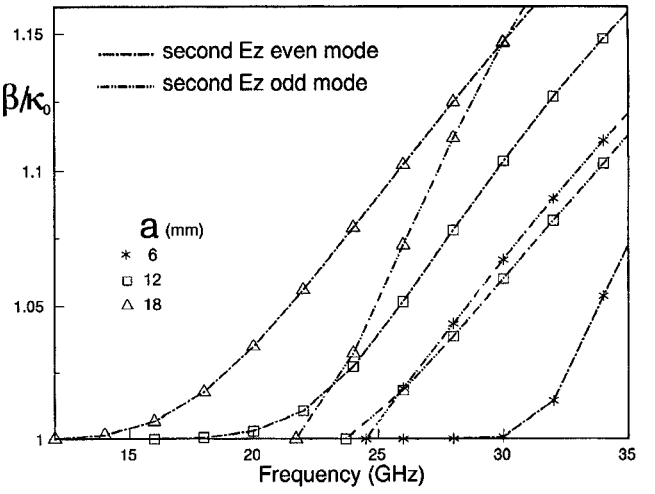

Fig. 5. Propagation constants of the second E_z even and odd modes as a function of frequency for different values of a ($\varepsilon_{r1} = \varepsilon_{r2} = 2.04$, $h_1 = 1$ mm, $h_2 = 2$ mm, $w_2 = 1.5$ mm, $s_2 = 1$ mm).

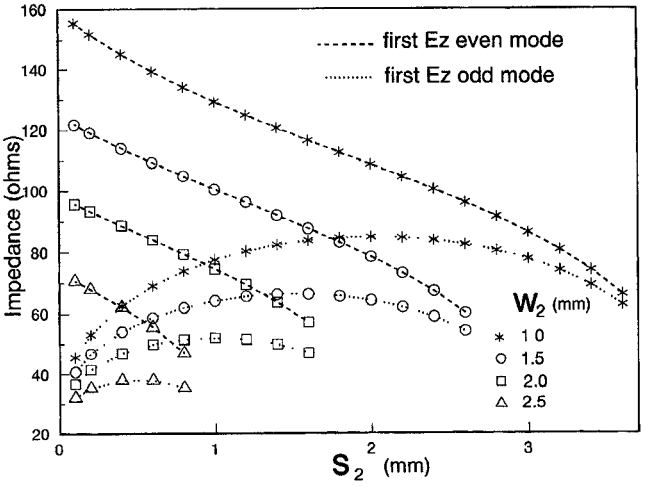

Fig. 6. Characteristic impedances of the fundamental modes as a function of s_2 for different values of w_2 ($\varepsilon_{r1} = \varepsilon_{r2} = 2.04$, $a = 6$ mm, $h_1 = 1$ mm, $h_2 = 2$ mm, $f = 10$ GHz).

of the second E_z even and odd modes are shown in Figs. 4 and 5 as a function of frequency for different values of groove height h and groove width a, respectively. It is apparent that decreasing the groove height and width can increase the cut-off frequency of the first higher-order mode, resulting in a wider fundamental mode bandwidth. It is also noted that the cutoff frequencies of second E_z odd and even modes are more strongly affected by h and a, respectively. Also shown in Fig. 3 are characteristic impedances of fundamental modes as a function of frequency. It is seen that in the fundamental-mode frequency range, the propagation constants and characteristic impedances change very little with increasing frequency. Such a low dispersion characteristic is useful for some broad-band applications.

Fig. 6 shows characteristic impedances of two fundamental modes as a function of width of the gap between two strips s_2 for different values of strip width w_2. It is apparent that a wide range of characteristic impedances can be obtained by changing s_2 and w_2. As s_2 is decreased, the characteristic impedance of the E_z even mode increases; but the characteristic impedance of the E_z odd mode increases first, and then decreases after reaching a maximum value. As expected, with decreasing s_2, the difference between even and odd mode impedances becomes bigger. This results in stronger coupling between the two strips.

As seen from Fig. 6, the characteristic impedances of fundamental modes decrease by increasing w_2. The impedances can also be decreased by increasing the relative permittivities of two dielectric layers in the groove, as found from other obtained numerical results. The effect of increasing height ratio between two layers h_1/h_2 is also found to decrease the impedances, as seen from Fig. 7. But, with increasing h_1/h_2, the difference between even and odd mode impedances is decreased, resulting in weaker coupling. The reason for this is that as h_1/h_2 is increased, the field is more concentrated between strips and the base of the groove, resulting in less interaction between the two strips. Fig. 8 shows characteristic impedances as a function of a for different values of h. The decrease in a and h is found to decrease the characteristic impedance of the E_z even mode. The effect is more pronounced for the small values of a and h. However, the effect of changing a and h on the impedance of the E_z

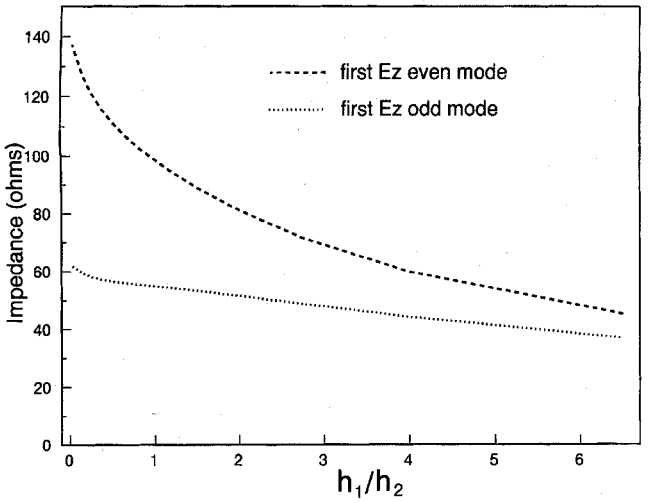

Fig. 7. Characteristic impedances of the fundamental modes as a function of h_1/h_2 ($\varepsilon_{r1} = \varepsilon_{r2} = 2.04$, $a = 6$ mm, $h = 3$ mm, $w_2 = 1.5$ mm, $s_2 = 0.5$ mm, $f = 10$ GHz).

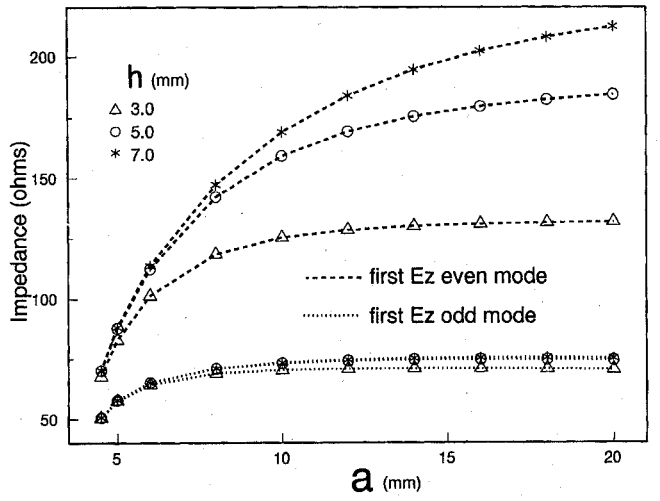

Fig. 8. Characteristic impedances of the fundamental modes as a function of a for different values of h ($\varepsilon_{r1} = \varepsilon_{r2} = 2.04$, $h_1 = 1$ mm, $w_2 = 1.5$ mm, $s_2 = 1$ mm, $f = 5$ GHz).

odd mode is very small since the field for this mode is concentrated in the region between two strips. Since there are many parameters that can be chosen, as mentioned above, any desired values of impedances of two fundamental modes and the difference between them can be achieved.

In the fundamental mode frequency range, the characteristics of two fundamental modes can be used to design a directional coupler. It is clearly seen from Fig. 3 that the difference between propagation constants of these two modes is small. This can lead to high directivity. However, to achieve complete isolation for the isolated port, propagation constants of the two modes should be the same. This is possible at certain frequencies for this structure by using different permittivities for two dielectric layers, as seen from Fig. 9 which shows propagation constants of two fundamental modes for different values of ε_{r1}. It is also found that when $\varepsilon_{r1} = \varepsilon_{r2}$, the propagation constant of the first odd mode is bigger than that of the first even mode; but when $\varepsilon_{r1} = 1$, the propagation constant of the odd mode is smaller. Therefore, to achieve the same propagation constants for

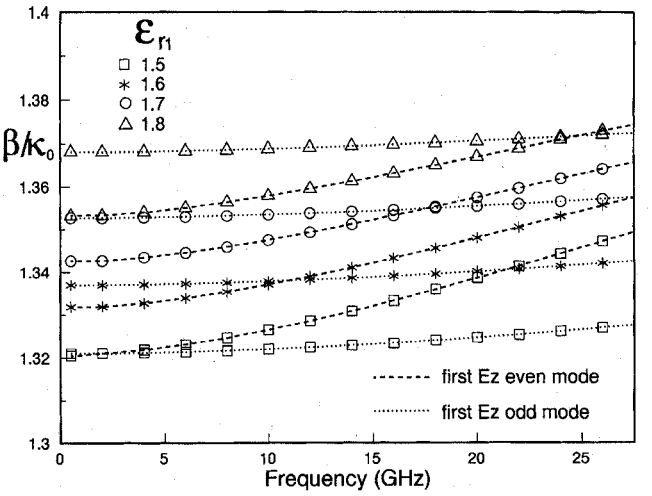

Fig. 9. Propagation constants of the fundamental modes as a function of frequency for different values of ε_{r1} ($\varepsilon_{r2} = 2.04$, $a = 6$ mm, $h_1 = 1$ mm, $h_2 = 2$ mm, $w_2 = 1.5$ mm, $s_2 = 1$ mm).

these two modes, ε_{r1} should be properly chosen to be between 1 and ε_{r2}.

IV. Conclusion

Potential advantages of the edge coupled strip IDG have been identified, and they could be useful in microwave and millimeter wave applications. The extended spectral domain approach has been used for the analysis of this structure. Accuracy of the analysis has been verified by comparison with measured data. It has been found that by decreasing the IDG dimensions, the fundamental mode frequency range can be widened. Also, the dispersion in propagation constants and characteristic impedances has been found to be very small in this frequency range. By suitable choice of the seven available parameters (five structural dimensions and two permittivities of two dielectric layers in the groove), a wide range of impedances of two fundamental modes and the difference between them can be achieved, leading to great flexibility in circuit design. Furthermore, the propagation constant of the first odd mode can be made equal to that of the first even mode by using different permittivities of two layers in the groove. This makes this structure very appropriate for the design of directional couplers with high directivity and good input match.

References

[1] D. A. Williams, "Millimeter-wave components and subsystems built using microstrip technology," *IEEE Trans. Microwave Theory Tech.*, vol. 39, pp. 768–774, May 1991.

[2] W. P. Harokopus, L. P. B. Katehi, W. Y. Ali-Ahmad, and G. M. Rebeiz, "Surface wave excitation from open microstrip discontinuities," *IEEE Trans. Microwave Theory Tech.*, vol. 39, pp. 1098–1107, July 1991.

[3] T. Rozzi and S. J. Hedges, "Rigorous analysis and network modeling of the inset dielectric guide," *IEEE Trans. Microwave Theory Tech.*, vol. 35, pp. 823–833, Sept. 1987.

[4] T. Rozzi, A. Morini, and G. Gerini, "Analysis and applications of microstrip loaded inset dielectric waveguide," *IEEE Trans. Microwave Theory Tech.*, vol. 40, pp. 272–278, Feb. 1992.

[5] T. Rozzi, G. Gerini, A. Morini, and M. Santis, "Multilayer buried microstrip inset guide," in *Proc. 21th European Microwave Conf.*, Stuttgart, 1991, pp. 673–678.

[6] N. Izzat, S. R. Pennock, and T. Rozzi, "Space domain analysis of micro-IDG structures," *IEEE Trans. Microwave Theory Tech.*, vol. 42, pp. 1074–1078, June 1994.

[7] Z. Fan and S. R. Pennock, "Broadside coupled strip inset dielectric guide and its directional coupler application," *IEEE Trans. Microwave Theory Tech.*, vol. 43, pp. 612–619, Mar. 1995.